



ELSEVIER

Available online at [www.sciencedirect.com](http://www.sciencedirect.com)

SCIENCE @ DIRECT®

Nuclear Instruments and Methods in Physics Research A 532 (2004) 622–630

**NUCLEAR  
INSTRUMENTS  
& METHODS  
IN PHYSICS  
RESEARCH**  
Section A

[www.elsevier.com/locate/nima](http://www.elsevier.com/locate/nima)

## Time–energy relation of the n\_TOF neutron beam: energy standards revisited

G. Lorusso<sup>a</sup>, N. Colonna<sup>a,\*</sup>, S. Marrone<sup>a</sup>, G. Tagliente<sup>a</sup>, M. Heil<sup>b</sup>, D. Cano-Ott<sup>c</sup>, M. Mosconi<sup>b</sup>, C. Moreau<sup>d</sup>, A. Mengoni<sup>e</sup>, U. Abbondanno<sup>d</sup>, G. Aerts<sup>f</sup>, H. Alvarez-Pol<sup>d</sup>, F. Alvarez-Velarde<sup>c</sup>, S. Andriamonje<sup>f</sup>, J. Andrzejewski<sup>g</sup>, A. Angelopoulos<sup>h</sup>, P. Assimakopoulos<sup>i</sup>, G. Badurek<sup>j</sup>, P. Baumann<sup>k</sup>, F. Bečvář<sup>l</sup>, J. Benlliure<sup>m</sup>, E. Berthomieux<sup>f</sup>, E. Bisceglie<sup>a</sup>, P. Calviño<sup>n</sup>, R. Capote<sup>o</sup>, P. Cennini<sup>e</sup>, V. Chepel<sup>p</sup>, E. Chiaveri<sup>e</sup>, C. Coceva<sup>q</sup>, G. Cortes<sup>n</sup>, D. Cortina<sup>m</sup>, A. Couture<sup>r</sup>, J. Cox<sup>r</sup>, S. Dababneh<sup>b</sup>, M. Dahlfors<sup>e</sup>, S. David<sup>s</sup>, R. Dolfini<sup>t</sup>, C. Domingo-Pardo<sup>u</sup>, I. Duran<sup>m</sup>, C. Eleftheriadis<sup>v</sup>, M. Embid-Segura<sup>c</sup>, L. Ferrant<sup>s</sup>, A. Ferrari<sup>e</sup>, R. Ferreira-Marques<sup>p</sup>, H. Fraiss-Koelbl<sup>w</sup>, W.I. Furman<sup>x</sup>, I.F. Goncalves<sup>y</sup>, E. Gonzalez-Romero<sup>c</sup>, A. Goverdovski<sup>z</sup>, F. Gramegna<sup>aa</sup>, E. Griesmayer<sup>w</sup>, F. Gunsing<sup>f</sup>, B. Haas<sup>ab</sup>, R. Haight<sup>ac</sup>, A. Herrera-Martinez<sup>e</sup>, K.G. Ioannides<sup>i</sup>, S. Isaev<sup>s</sup>, E. Jericha<sup>j</sup>, F. Käppeler<sup>b</sup>, Y. Kadi<sup>e</sup>, D. Karamanis<sup>i</sup>, V. Ketlerov<sup>z</sup>, G. Kitis<sup>v</sup>, P.E. Koehler<sup>ac</sup>, V. Konovalov<sup>z</sup>, E. Kossionides<sup>ad</sup>, M. Krτικά<sup>l</sup>, H. Leeb<sup>j</sup>, A. Lindote<sup>p</sup>, M.I. Lopes<sup>p</sup>, M. Lozano<sup>o</sup>, S. Lukic<sup>k</sup>, J. Marganec<sup>g</sup>, P.F. Mastinu<sup>aa</sup>, P.M. Milazzo<sup>d</sup>, A. Molina-Coballes<sup>o</sup>, F. Neves<sup>p</sup>, H. Oberhummer<sup>j</sup>, S. O'Brien<sup>r</sup>, J. Pancin<sup>f</sup>, C. Paradela<sup>m</sup>, A. Pavlik<sup>ae</sup>, P. Pavlopoulos<sup>af</sup>, L. Perrot<sup>f</sup>, V. Peskov<sup>ag</sup>, R. Plag<sup>b</sup>, A. Plompen<sup>ah</sup>, A. Plukis<sup>f</sup>, A. Poch<sup>n</sup>, A. Policarpo<sup>p</sup>, C. Pretel<sup>n</sup>, J.M. Quesada<sup>o</sup>, W. Rapp<sup>b</sup>, T. Rauscher<sup>ai</sup>, R. Reifarh<sup>aj</sup>, M. Rosetti<sup>q</sup>, C. Rubbia<sup>t</sup>, G. Rudolf<sup>ak</sup>, P. Rullhusen<sup>ah</sup>, J. Salgado<sup>y</sup>, E. Savvidis<sup>v</sup>, J.C. Soares<sup>y</sup>, C. Stephan<sup>s</sup>, J.L. Tain<sup>u</sup>, L. Tassan-Got<sup>s</sup>, L.M.N. Tavora<sup>y</sup>, R. Terlizzi<sup>a</sup>, N. Tsangas<sup>ak</sup>, G. Vannini<sup>al</sup>, P. Vaz<sup>y</sup>, A. Ventura<sup>q</sup>, D. Villamarin<sup>c</sup>, M.C. Vincente<sup>c</sup>, V. Vlachoudis<sup>e</sup>, R. Vlastou<sup>h</sup>, F. Voss<sup>b</sup>, H. Wendler<sup>e</sup>, M. Wiescher<sup>r</sup>, K. Wisshak<sup>b</sup>

<sup>a</sup> *Istituto Nazionale di Fisica Nucleare - Sezione di Bari, via Amendola 173, I-70126 Bari, Italy*

<sup>b</sup> *Forschungszentrum Karlsruhe GmbH, Institut für Kernphysik, Karlsruhe, Germany*

<sup>c</sup> *Centro de Investigaciones Energéticas Medioambientales y Tecnológicas, Madrid, Spain*

<sup>d</sup> *Istituto Nazionale di Fisica Nucleare - Sezione di Trieste, Italy*

<sup>e</sup> *CERN, Geneva, Switzerland*

<sup>f</sup> *CEA/Saclay - DSM/DAPNIA/SPhN, Gif-sur-Yvette, France*

<sup>m</sup> *Universidad de Santiago de Compostela, Spain*

\*Corresponding author. Tel.: +39-80-544 2351; fax: +39-80-544 2740.

E-mail address: [nicola.colonna@ba.infn.it](mailto:nicola.colonna@ba.infn.it) (N. Colonna).

- <sup>g</sup> University of Łódź, Łódź, Poland  
<sup>h</sup> Astro-Particle Consortium, University of Athens, Greece  
<sup>i</sup> Astro-Particle Consortium, University of Ioannina, Greece  
<sup>j</sup> Atominstitut der Österreichischen Universitäten, Technische Universität Wien, Austria  
<sup>k</sup> Centre National de la Recherche Scientifique IN2P3 - IreS, Strasbourg, France  
<sup>l</sup> Charles University, Prague, Czech Republic  
<sup>n</sup> Universitat Politècnica de Catalunya, Barcelona, Spain  
<sup>o</sup> Universidad de Sevilla, Spain  
<sup>p</sup> Laboratório de Instrumentação e Física Experimental de Partículas, Coimbra, Portugal  
<sup>q</sup> ENEA, Bologna, Italy  
<sup>r</sup> University of Notre Dame, USA  
<sup>s</sup> Centre National de la Recherche Scientifique IN2P3 - IPN, Orsay, France  
<sup>t</sup> Università degli Studi Pavia, Italy  
<sup>u</sup> Instituto de Física Corpuscular, CSIC-Univ. Valencia, Spain  
<sup>v</sup> Astro-Particle Consortium, University of Thessaloniki, Greece  
<sup>w</sup> Fachhochschule Wiener Neustadt, Wien, Austria  
<sup>x</sup> Joint Institute for Nuclear Research, Frank Laboratory of Neutron Physics, Dubna, Russia  
<sup>y</sup> Instituto Tecnológico e Nuclear, Lisboa, Portugal  
<sup>z</sup> Institute of Physics and Power Engineering, Obninsk, Russia  
<sup>aa</sup> Istituto Nazionale di Fisica Nucleare, Laboratori Nazionali di Legnaro, Italy  
<sup>ab</sup> CEN, Bordeaux-Gradignan, France  
<sup>ac</sup> Oak Ridge National Laboratory, Physics Division, Oak Ridge, USA  
<sup>ad</sup> Astro-Particle Consortium, NCSR “Demokritos”, Athens, Greece  
<sup>ae</sup> Institut für Isotopenforschung und Kernphysik, Universität Wien, Austria  
<sup>af</sup> Pole Universitaire Leonard de Vinci, Paris La Defense, Cedex, France  
<sup>ag</sup> Kungliga Tekniska Hogskolan, Physics Department, Stockholm, Sweden  
<sup>ah</sup> CEC-JRC-IRMM, Geel, Belgium  
<sup>ai</sup> University of Basel, Switzerland  
<sup>aj</sup> Los Alamos National Laboratory, New Mexico, USA  
<sup>ak</sup> Astro-Particle Consortium, University of Thrace, Greece  
<sup>al</sup> Dipartimento di Fisica and INFN, Bologna, Italy

Received 14 April 2004; accepted 26 April 2004

Available online 8 July 2004

The n\_TOF Collaboration

---

## Abstract

The accurate determination of neutron cross-sections as a function of the neutron energy at a time-of-flight facility requires a precise knowledge of the time–energy relation for the neutron beam. For the n\_TOF neutron beam at CERN, produced by spallation of high-energy protons on a Pb target, the time–energy relation is connected to the production mechanism and to the subsequent moderation process. A calibration of the neutron energy scale is proposed based on detailed Monte Carlo simulations of the facility. This time–energy relation has been experimentally validated by means of dedicated measurements of standard energy resonances, from 1 eV to approximately 1 MeV. On the basis of the present measurements, it is proposed to correct the energy of the 1.3 eV resonance of <sup>193</sup>Ir, which is commonly considered as an energy standard.

© 2004 Elsevier B.V. All rights reserved.

PACS: 25.40.Lw; 25.40.Ny; 29.40.Mc; 29.25.Dz; 06.20.Fn

Keywords: Spallation neutron source; Moderation distance; Neutron capture cross sections; Neutron energy standards

---

## 1. Introduction

The need of high-quality neutron cross-section data, in particular for actinides and radioactive-fission products, has recently prompted the construction of a novel neutron time-of-flight facility, n\_TOF, at CERN [1]. The neutron beam is generated via spallation of Pb by 20 GeV/c protons, and subsequent moderation in a 5 cm thick layer of cooling water, surrounding the spallation target. Neutrons emerging in the forward direction, propagate through a vacuum tube to the experimental area, located approximately 185 m downstream. Two collimators and several concrete and iron shielding walls are placed along the path in the time-of-flight tunnel. The main characteristics of the facility, that are extremely high instantaneous neutron flux, the excellent energy resolution and the broad neutron energy range, allow high precision measurements for a variety of isotopes, especially for radioactive ones, which is of interest both for Nuclear Astrophysics [2] and for application to emerging nuclear technologies, in particular for the design of Accelerator Driven Systems for nuclear waste transmutation [3].

The measurements, planned or currently performed at n\_TOF, aim at studying cross-sections as a function of neutron energy. Since the spallation source provides a white neutron beam, the quality of the measurement strongly depends on the determination of the neutron energy, which must be reconstructed from the measured time-of-flight. Hence, a precise knowledge of the time–energy relation is mandatory to obtain high-accuracy cross-sections data at all energies.

As for all spallation facilities, the effective length of the flight path at n\_TOF is the sum of the geometrical length, defined as the distance between the outer face of the moderator and the reaction sample, plus the “moderation distance”, that is the effective distance covered by the neutron during the moderation process inside the spallation target and the water moderator [4]. Since one does not know the moderation distance for each detected neutron, an average value has to be used. This average and its energy dependence, can be inferred from detailed simulations of the spallation and

moderation processes, by generating a distance distribution for different neutron energies. Even though simulations can provide a realistic estimate of the effective length of the neutron flight path and its dependence on the neutron energy, these results need to be experimentally validated. To this end, a dedicated measurement campaign was performed at n\_TOF. In particular, the time–energy relation was determined in the range between 1 eV and 1 MeV, by means of several capture resonances, which are considered as neutron energy standards. After a discussion of the simulated time–energy relation, the experimental technique and the results obtained for the time–energy relation of the n\_TOF neutron beam are presented. The present results imply a revision of the energy of one of the commonly used standard resonances.

## 2. Simulations

At a time-of-flight facility, the absolute neutron energy can be determined from the length of the flight path and from the flight time, via the relation

$$E = \left( \frac{72.2977 L}{t} \right)^2 \quad (1)$$

where  $E$  (in eV) is the nonrelativistic neutron energy,  $L$  is the effective flight path in meters and the flight time  $t$  is expressed in  $\mu\text{s}$ . Above a few keV, relativistic corrections, or directly the relativistic expression, should be used.

At a spallation neutron source, the effective length of the flight-path is influenced by the moderation process, which results in an additional distance to be added to the geometrical flight base. For convenience, one can express the effective length  $L$  as the sum of a fixed length  $L_0$  and an energy-dependent term  $\Delta L$  (it should be noted that  $L_0$  represents the geometrical length plus the energy-independent term of the moderation distance). In the case of the n\_TOF neutron beam, the energy-dependent term of the moderation distance  $\Delta L$  has been studied by means of Monte Carlo simulations using the codes FLUKA and CAMOT (for consistency with experimental observables, the neutron path inside the target-moderator assembly

is evaluated from the moderation time at the final neutron energy, i.e.  $L_{mod} = vt_{mod}$ ; see Ref. [4] for more details). The mean of the simulated distribution of the moderation distance has been calculated for selected neutron energies. Fig. 1 shows the results of the simulations: the additional length  $\Delta L$ , and consequently the total flight-path length, increases as a function of neutron energy, up to several hundred keV, and then starts decreasing, as a consequence of the diminishing importance of the moderation process for higher energy neutrons.

The values of  $\Delta L$  obtained from the simulations can be expressed up to few hundred keV by the simple relation

$$\Delta L = 0.101 \sqrt{E} \quad (2)$$

where  $\Delta L$  is in cm and  $E$  is the neutron energy in eV.

The energy dependence of the flight-path length can be included in the time–energy relation through an iterative procedure: as a first step, the approximate neutron energy is calculated from the measured time-of-flight, by applying Eq. (1) with only the fixed term of the flight-path length (i.e.

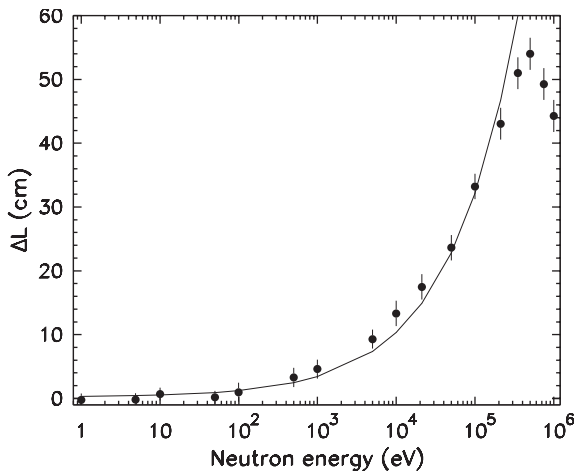


Fig. 1. The energy-dependent term of the average moderation distance for neutron energies between 1 eV and 1 MeV, extracted from FLUKA + CAMOT simulations (symbols) and fitted with Eq. (2) (solid curve). Above a few hundred keV,  $\Delta L$  starts deviating from the square-root dependence on the neutron energy. The energy-dependent term  $\Delta L$  has to be added to the fixed term  $L_0$ , to obtain the correct time–energy relation.

$L_0$ ). With this approximate neutron energy, the additional length  $\Delta L$  is then calculated, by applying the appropriate energy dependence (for example Eq. (2)). Finally, the accurate neutron energy is calculated with Eq. (1), using now  $L = L_0 + \Delta L$  the total, effective length of the flight path.

A more convenient way to calculate the neutron energy can be used if  $\Delta L$  varies with the square root of the neutron energy, as predicted from the simulations in the case of the n\_TOF neutron beam. In fact, it can be shown from Eq. (1) that the addition of a suitably chosen offset  $t_0$  on the measured time-of-flight corresponds to an additional flight-path  $\Delta L$  according to the following expression:

$$\Delta L = -\frac{\sqrt{E}}{72.2977} t_0 \quad (3)$$

(note that an increase in the flight-path length corresponds to a negative  $t_0$ ). In this assumption, the neutron energy can be immediately calculated from Eq. (1), without a second iteration, with the fixed flight-path length  $L_0$ , and with the time  $t$  given by the measured time-of-flight plus an experimentally determined  $t_0$ . For the n\_TOF neutron beam, the value of  $t_0$  predicted on the basis of the Monte Carlo simulations can be estimated, by comparing Eqs. (2) and (3), to be approximately  $-73$  ns.

In light of these considerations, an experimental calibration of the time–energy relation for the n\_TOF neutron beam reduces to the determination of the fixed flight-path length  $L_0$  and of a suitable offset on the time-of-flight,  $t_0$ .

### 3. Experimental time-to-energy calibration

The time–energy relation for the n\_TOF neutron beam was studied by measuring specific cross-section resonances, adopted as energy standards [5,6]. To be used for this purpose, the resonances need to be narrow and symmetric, and their energy to be known with very high accuracy, typically below one per thousand. The time–energy relation was investigated in the typical energy range of capture reactions, between 1 eV

and approximately 1 MeV, by measuring the three reactions:  $^{193}\text{Ir}(n,\gamma)$ ,  $^{238}\text{U}(n,\gamma)$  and  $^{32}\text{S}(n,\gamma)$ . Table 1 lists the resonances in the capture cross-sections for the three samples, used as energy standards in the present analysis.

The experimental apparatus used in the measurement consisted in two liquid scintillator  $\text{C}_6\text{D}_6$  detectors, optimized for low neutron sensitivity [7]. The samples were mounted on a sample-changer in air, with 75  $\mu\text{m}$  thick mylar windows at the vacuum-air interface. Very thin samples of  $^{238}\text{U}$  and  $^{193}\text{Ir}$  were used, while for  $^{32}\text{S}$  the sample thickness was approximately 1 mm. The detector signals were recorded with fast Flash ADCs of the standard n-TOF acquisition system [8].

The Pulse Height Weighting Technique was applied for all resonances, except the highest in energy, in order to obtain the capture yield [9]. The energy calibration of the  $\text{C}_6\text{D}_6$  detectors was performed by means of  $^{137}\text{Cs}$ ,  $^{60}\text{Co}$  and Pu/C  $\gamma$ -ray sources. The neutron energy is calculated according to Eq. (1) and its relativistic extension, using the time-of-flight measured relative to the proton beam pulse, based on the reference signal provided by the prompt  $\gamma$ -flash detected in the  $\text{C}_6\text{D}_6$  detectors.

For the determination of the capture yield, the n-TOF neutron flux, measured with a calibrated fission chamber, was used [10]. The integrated neutron fluence was estimated from the total number of protons impinging on the spallation target. The background was not subtracted from

the yield, but treated as a free parameter in the resonance analysis.

The resonances in the capture yield for the three samples were analyzed with the multi-level analysis code SAMMY [11]. For all considered resonances, the neutron and gamma widths were fixed to the tabulated values of Refs. [12,13], or allowed to vary within the tabulated uncertainty. The energy of the resonance, the normalization factor and the background level were kept as free parameters. While for the  $^{193}\text{Ir}$  and  $^{238}\text{U}$  resonances, the measured resonance width is affected mainly by Doppler broadening, the analysis of the  $^{32}\text{S}$  resonances required a careful consideration of the energy resolution of the n-TOF neutron beam, which becomes important for narrow resonances above a few keV. In the present analysis, the RPI resolution function, included in the standard release of the SAMMY code was used. This function, consisting of a  $\chi^2$  function and two exponential terms, was chosen since it reproduces reasonably well the broadening related to the moderation process for the n-TOF installation. The parameters of the RPI function have been determined from a systematic analysis of Monte Carlo simulations of the spallation and moderation processes, for different neutron energies [14]. In order to reproduce the shape of the measured resonances, two out of the nine parameters of the RPI function, that is the width of the  $\chi^2$  distribution and the normalization of the two exponential terms, were allowed to vary within the estimated 20% uncertainty related to the parameterization of the simulated resolution functions. By choosing the corresponding option in SAMMY, the resonance energy was determined as the centroid of the fitting distribution, in order to allow for a meaningful comparison with the results of the simulations, discussed in Section 2.

Figs. 2–4 show the yield for the standard energy resonances measured for the three capture reactions. The curves represent the results of the SAMMY R-matrix analysis. Since the expected energy dependence of the term  $\Delta L$  starts becoming important only above a few keV, the low-energy  $^{193}\text{Ir}$  and  $^{238}\text{U}$  resonances were first analyzed in order to determine the energy-independent term,  $L_0$ , in the flight-path length (according to Eq. (2),

Table 1

The resonances, considered as energy standards, used in this work for energy calibration of the n-TOF neutron beam. The capture and neutron widths of the resonances are also included in the table

Reaction	$E$	$\Gamma_\gamma$	$g\Gamma_n$
$^{193}\text{Ir}(n,\gamma)$	1.298(1) eV	83.3(80) meV	0.421(5) meV
$^{238}\text{U}(n,\gamma)$	6.673(1) eV	23.4(3) meV	1.49(2) meV
$^{238}\text{U}(n,\gamma)$	20.864(3) eV	22.5(8) meV	10.2(2) meV
$^{238}\text{U}(n,\gamma)$	36.671(6) eV	23.5(3) meV	33.8(2) meV
$^{238}\text{U}(n,\gamma)$	66.015(10) eV	23.7(1) meV	24(1) meV
$^{32}\text{S}(n,\gamma)$	30.388(23) keV	1.01(50) eV	0.0636(11) keV
$^{32}\text{S}(n,\gamma)$	97.550(7) keV	0.323(23) eV	0.234(4) keV
$^{32}\text{S}(n,\gamma)$	513.33(10) keV	3.10(28) eV	0.024(5) keV
$^{32}\text{S}(n,\gamma)$	819.34(18) keV	0.41(11) eV	1.69(20) keV

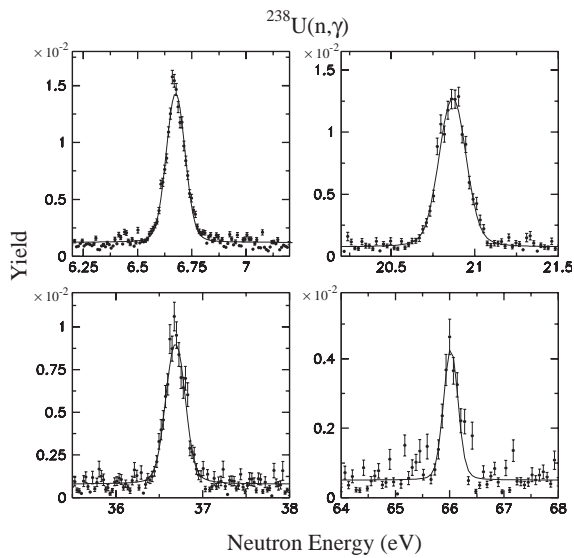


Fig. 2. Measured standard energy resonances of  $^{238}\text{U}(n,\gamma)$ . The solid symbols represent the yield measured at n\_TOF, while the solid lines are the result of a resonance analysis performed with SAMMY (see text for more details).

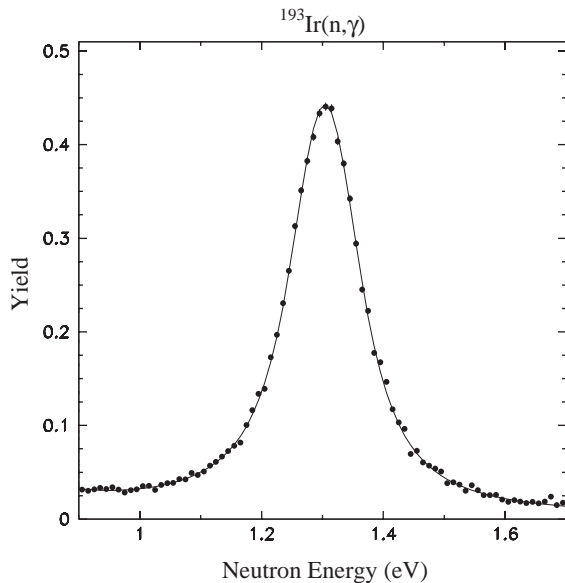


Fig. 3. Measured standard energy resonance of the  $^{193}\text{Ir}(n,\gamma)$  reaction (solid symbols), and result of SAMMY resonance analysis (line).

$\Delta L$  amounts to less than 3 cm at 800 eV, which corresponds to a relative contribution of  $1.6 \times 10^{-4}$ , a value comparable to the uncertainty

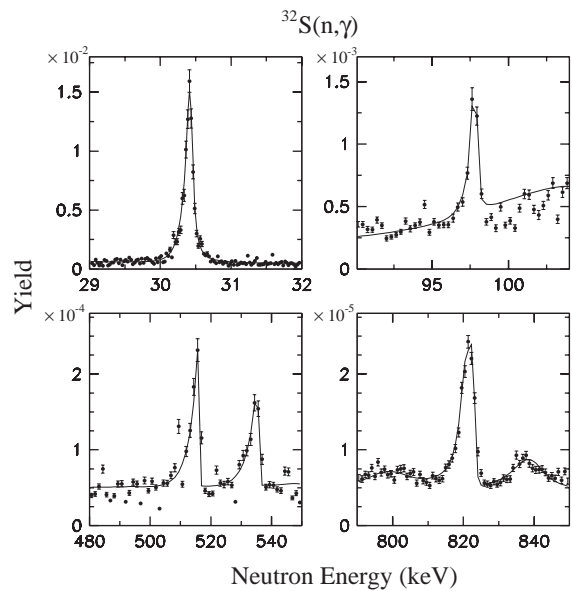


Fig. 4. Measured standard energy resonances for the  $^{32}\text{S}(n,\gamma)$  reaction. The SAMMY analyses are indicated by the solid lines.

of the present analysis). From the analysis of the  $^{238}\text{U}$  resonances, shown in Fig. 2, a value of  $185.20 \pm 0.01$  m has been derived for  $L_0$  (whereas the geometrical distance of the sample from the exit window of the spallation target is 185.05 m). With this value, the energy of all considered resonances of  $^{238}\text{U}$  agreed with the standard values within the quoted uncertainties.

When using the value of  $L_0$  determined from the  $^{238}\text{U}$  standard resonances, a discrepancy is observed for the 1.298 eV resonance of  $^{193}\text{Ir}$ . The SAMMY fit, shown in Fig. 3, yields an energy of 1.3047(3) eV for this resonance. This result is 0.54% higher than the adopted standard energy, much higher than the uncertainty quoted for the standard energy, as well as that estimated for the present measurement. More importantly, the difference between the measured and tabulated values for the resonance energy is incompatible with the results obtained for the  $^{238}\text{U}(n,\gamma)$  reaction. In fact, a change in the length of the flight-path, to account for the observed difference in the  $^{193}\text{Ir}$  resonance, would result in systematically higher energies for all measured  $^{238}\text{U}$  resonances than are tabulated. Therefore, it was concluded that the energy of the  $^{193}\text{Ir}$  resonance may be

affected by a systematic error, and should be revised. To further investigate this issue, we considered all currently available measurements for this resonance, shown in Table 2 [15]. As can be noted, only one of the measurements (Fisher et al.) has reported a value of 1.298 eV, although with a very small uncertainty. All other measurements indicate an energy close to the 1.305 eV obtained in our analysis. Possibly, an unknown systematic uncertainty in the measurement of Fisher et al., may have led to this discrepancy. Our result clearly yields a higher energy for this resonance of  $^{193}\text{Ir}$ , and indicates the need for a revision of this standard. Because of this discrepancy, it was decided to disregard the  $^{193}\text{Ir}(n,\gamma)$  measurement in the time–energy calibration.

Having determined the fixed term of the flight path from the  $^{238}\text{U}(n,\gamma)$  resonances, the capture reaction of  $^{32}\text{S}$  was studied to characterize the energy-dependent term  $\Delta L$  or equivalently, the offset  $t_0$  in time-of-flight. Several well-resolved resonances in the  $^{32}\text{S}(n,\gamma)$  reaction, included in the list of energy standards, can be used to cover a broad energy range, from a few keV to approximately 1 MeV, and are therefore appropriate to study the time–energy relation. The resonances used in the present analysis are shown in Fig. 4, together with the results of SAMMY fits. Contrary to the low-energy resonances, for which the Doppler broadening dominates, the energy resolution of the beam becomes important above a few keV, and affects the extracted resonance widths. Consequently, the shape of the resonance deviates from a Breit–Wigner form, and becomes more asymmetric, with a low-energy tail which affects the determination of the resonance energy. Fig. 4

Table 2  
The existing measurements of the 1.3 eV resonance of the  $^{193}\text{Ir}(n,\gamma)$  reaction

Resonance energy (eV)	Author (from EXFOR file)
1.303(5)	H.H. Landon (1955)
1.301(3)	J. Brunner, et al. (1967)
1.3070(25)	V.P. Vertebnyj, et al. (1980)
1.298(1)	P. Fisher, et al. (1982)
1.304(4)	S.M. Masyanov, et al. (1992)

shows that the shape of the resonances is well reproduced with the RPI resolution function adopted for n\_TOF, thus providing confidence in the extracted resonance energies.

A discrepancy was observed for the neutron width of the resonance at 30.388 keV. In Ref. [12], this resonance is assigned an orbital angular momentum  $l=1$  and a total spin  $J=\frac{1}{2}$ . In the present analysis, it is found that, while  $g\Gamma_n$  agrees perfectly with the tabulated value, the assumption of  $J=\frac{1}{2}$  leads to a neutron width half of the tabulated one. On the contrary, both  $g\Gamma_n$  and  $\Gamma_n$  agree with previous measurements if  $J=\frac{3}{2}$  is used.

The first column of Table 3 reports the energy of the resonances measured in the present work, obtained with a fixed flight-path length of 185.2 m. The second column shows the deviation from the standard value, reported in Ref. [13]. This discrepancy is still small at 30 keV, but increases up to almost one percent at higher energies. This clearly indicates an energy dependence in the length of the flight-path. As an example, good agreement (within 0.1% for most resonances) is obtained if one keeps the value of  $L_0=185.2$  m in the energy range 1 eV to 400 keV, and changes to  $L_0=185.5$  m in the energy range 400 keV–1 MeV.

As previously mentioned, an additional length in the flight path varying with the square root of the neutron energy can be replaced by a suitable offset in time-of-flight. In this case, the resonance

Table 3  
Energy of standard resonances measured at n\_TOF, calculated with a fixed length of the flight-path ( $L_0=185.2$  m).

$E_{\text{Fit}}$	Deviation from standard value (%)	$\Delta L$ (cm)
1.3047(3) eV	0.5	–46.3
6.6752(6)	–0.03	2.8
20.865(2)	0.005	–0.5
36.678(4)	0.02	–1.9
66.02(1)	0.01	–0.9
30.330(2) keV	–0.19	17.6
97.29(6)	–0.26	24.1
509.256(24)	–0.8	74.1
811.47(4)	–0.97	89.8

The deviations of the measured resonances from the standard values are listed in the second column. The corresponding additional flight-path length  $\Delta L$  is reported in the third column.

energies vary according to

$$dE \propto E^{3/2} dt_0 \quad (4)$$

where  $t_0$  represents the time off-set.

The optimal value of the time offset has been determined by minimizing the root mean square deviation of the measured energy from the tabulated values for the  $^{32}\text{S}$  resonances used in the present analysis. Fig. 5 shows the remaining deviations from the standard values after applying a correction of  $t_0 = -68 \pm 13$  ns (solid symbols and solid line). For comparison, the open symbol shows the deviation of the energy obtained by using the standard value for the  $^{193}\text{Ir}$  resonance. The need of a reduction of this resonance energy by 0.5% is evident.

As previously mentioned, the addition of a negative offset corresponds to an additional length in the flight path, which varies with the square root of the neutron energy. Therefore, the present results can be directly compared with the results of the Monte Carlo simulations with FLUKA and CAMOT, in Fig. 1 [4]. In particular, the experimentally determined value of  $t_0$  leads to

$$\Delta L = (0.094 \pm 0.018) \sqrt{E}.$$

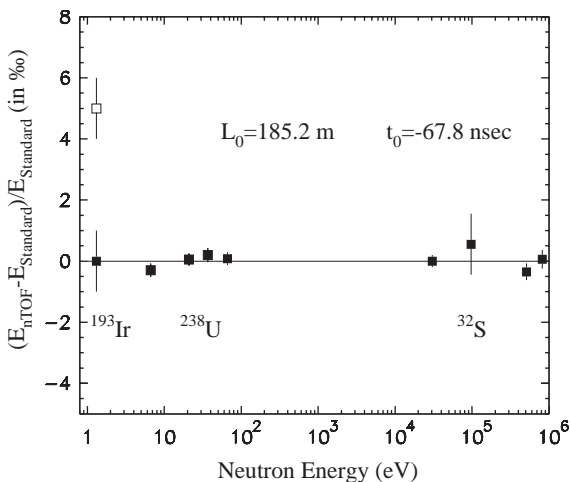


Fig. 5. Deviation of the energy of the standard resonances measured at n.TOF from the values tabulated in Refs. [12,13] after applying the correct time–energy relation and considering a revised energy for the  $^{193}\text{Ir}$  resonance (black squares). The deviation of the measured energy of this resonance from the tabulated value is indicated by the open square.

The agreement with the predicted trend of Eq. (2) is striking, and confirms the correctness of the simulations in an energy region where the effect of the moderation process is dominant.

#### 4. Conclusions

The time–energy calibration of the n.TOF neutron beam has been performed by measuring the energy standard resonances in the capture cross-sections of  $^{193}\text{Ir}$ ,  $^{238}\text{U}$  and  $^{32}\text{S}$ . At low energy, where the energy dependence of the moderation distance is negligible, the length of the flight path has been determined from four resonance in the  $^{238}\text{U}(n,\gamma)$  reaction. The measurements of the 1.298 eV resonance in the  $^{193}\text{Ir}(n,\gamma)$  cross-section indicate that this standard needs to be revised to a value of  $1.3047 \pm 0.0003$  eV. In the keV energy range, the dependence of the moderation distance as a function of the neutron energy has been confirmed by means of the standard  $^{32}\text{S}$  resonances, as had been predicted by detailed simulations of the spallation and moderation process. A square-root dependence, or equivalently, an offset of the measured time-of-flight, has been proven to describe reliably both the simulations and the experimental results. In particular, the time–energy calibration performed by analysing the  $^{32}\text{S}$  resonances, indicates a value for the offset of  $-68 \pm 13$  ns, consistent with the simulations. Although the present results have been obtained in the energy range below 1 MeV, which is typical of capture reactions, they provide strong evidence for the accuracy of the simulations which, therefore, can be used also at higher energies.

#### Acknowledgements

This work was supported by the EC under the contract Nr. FIKW-CT-2000-00107.

#### References

- [1] The n.TOF Collaboration, Proposal for a neutron time-of-flight facility, CERN/SPSS 99-08, SPSC/P310, March 1999;



- “n\_TOF Technical Report”, CERN/INTC 2000-018, CERN, 2000.
- [2] F. Käppeler, F.K. Thielemann, M. Wiescher, *Ann. Rev. Nucl. Part. Sci.* 48 (1998) 175.
- [3] C. Rubbia, et al., CERN/AT/95-44, CERN, 1995; C.D. Bowman, *Ann. Rev. Nucl. Part. Sci.* 48 (1998) 505.
- [4] C. Coceva, et al., *Nucl. Instr. and Meth. A* 489 (2002) 346.
- [5] C. Coceva, et al., Neutron energy standards for white neutron sources, IAEA-TECDOC-410, Leningrad, USSR, 1986, p. 56.
- [6] C. Coceva, et al., Neutron energy standards, In: H. Condé (Ed.), *Nuclear data standards for nuclear measurements*, NEA-OECD Report, NEANDC-311”U”, INDC (SEC)-101, 1992, p. 83.
- [7] P. Plag, et al., *Nucl. Instr. and Meth. A* 496 (2003) 425.
- [8] R. Plag, et al., *Nucl. Instr. and Meth. A*, submitted.
- [9] U. Abbondanno, et al., *Nucl. Instr. and Meth. A* 521 (2004) 545.
- [10] C. Borcea, et al., *Nucl. Instr. and Meth. A* 513 (2003) 524.
- [11] N. Larsson, A code system for multilevel R-matrix fits to neutron data using Bayes equations, ORNL/TM-9179/R5, 2000.
- [12] S.F. Mughabghab, D.I. Garber, *Neutron Cross Sections: Neutron Resonance Parameters and Thermal Cross Sections*, Academic Press, New York, 1984.
- [13] S. Sukhoruchin, Z.N. Soroko, V.V. Deriglazov, in: *Tables of Neutron Resonance Parameters*, Landolt-Börnstein Series, Vol. 16, Springer, Berlin, 1998.
- [14] The n\_TOF Collaboration, Performance Report, CERN/INTC-2002-037, CERN, 2002.
- [15] The EXFOR database, Nuclear Reaction Data Center Network, IAEA-NDS-207 (BNL-NCS-63330-00/04-Rev.), <http://www-nds.iaea.org>.